WHY AND HOW TO MEASURE LIPID BILAYER THICKNESS?

P. Balgavý, balgavy@fpharm.uniba.sk, Faculty of Pharmacy, Comenius University, 832 32 Bratislava, J. Gallová, jana.gallova@fpharm.uniba.sk, Faculty of Pharmacy, Comenius University, Bratislava, J. Karlovská, janka.karlovska@fpharm.uniba.sk, Faculty of Pharmacy, Comenius University, 832 32 Bratislava, M. Kotalová, kotalova@gmail.com, Faculty of Mathematics, Physics and Informatics, Comenius University, 842 15 Bratislava, N. Kučerka, norbert.nucerka@nrc.gc.ca, Canadian Neutron Beam Centre, NRC, Chalk River, ON K0J 1P0, Canada, T. Murugova, tatiana.murugova@mail.ru, FLNP JINR, Dubna, Russia, J. Teixeira, teix@dsm-mail.saclay.cea.fr, Laboratoire Léon Brillouin (CEA-CNRS), CEA Saclay, France, D. Uhríková, uhrikova@fpharm.uniba.sk, Faculty of Pharmacy, Comenius University, 832 32 Bratislava

INTRODUCTION

Two major components of biological membranes are lipids and proteins [1]. Integral membrane proteins, which span the lipid bilayer, mediate the transport of matter and signals through bilayer. The function and properties of these proteins depend on bilayer structural and dynamical parameters [1]. Some of these parameters include various thicknesses, such as the hydrophobic thickness d_C, the polar headgroup region thickness d_H and the number of water molecules n_W located therein, and the steric thickness $d_S=d_C+2d_H$. The central structural quantity is the average area per lipid molecule A_L along the surface of the bilayer, to which thicknesses are related through volume considerations: $A_L=V_C/d_C=(V_H+n_WV_W)/d_H=2(V_L+n_WV_W)/d_S$, where $V_L=V_C+V_H$ and V_W is the molecular volume of lipid and water, respectively, and V_C and V_H the volumes of hydrophobic and polar part of the lipid molecule, respectively.

The bilayer thicknesses are studied using x-ray and neutron diffraction and scattering on models of the lipid part of biomembranes, e.g. on stacks of lipid bilayers organized in lamellar lyotropic liquid crystals, on curved concentric bilayers in multilamellar (onion-like) vesicles or in spherical unilamellar (hollow-sphere-like) vesicles. However, fluctuations inherent in flexible and biologically relevant fully hydrated fluid-like lipid bilayers make quantitative determination of these structural parameters difficult, because such bilayers have atomic distribution functions with widths spread over 0.5 nm. This precludes an atomic-level structural description and substantially limits the quality and quantity of structural data that can be obtained using classical diffraction methods. Recently, there has been some methological progress in this soft condensed matter field. One new development uses the diffuse synchrotron x-ray scattering from fully hydrated oriented bilayer stacks as a continuous function of the scattering vector q instead of the Bragg diffraction peaks to obtain the bilayer electron density profile from which structural parameters and bilayer elastic moduli are deduced [2,3]. The second approach to lipid bilayer structure that is the subject of the present contribution studies samples composed of unilamellar vesicles instead of multilamellar arrays. Unilamellar vesicles are attractive because they are topologically equivalent to cells with an aqueous interior and exterior. They have also advantages in studies of effects of various additives in bilayers.

Recently, we have developed advanced methods, inspired by molecular dynamics simulations, for analyzing data of small-angle neutron scattering (SANS) on unilamellar vesicles [4,5]. In the present contribution, some of our data obtained by SANS and these methods will be used to understand functional properties of an integral membrane protein, the sarcoplasmic reticulum Ca^{2+}-transporting ATPase (SERCA), isolated from rabbit skeletal muscles, purified and reconstituted into unilamellar vesicles from monounsaturated diacyl-phosphatidylcholines (diCn:1PC, n is the even number of acyl chain carbons). We study the effect of cholesterol (CHOL), an ubiquitous component of mammalian membranes, and the effect of *N*-dodecyl-*N*,*N*-dimethylamine-*N*-oxide (C12NO), a mild detergent used for the membrane protein isolation, reconstitution and crystallization, on both the SERCA activity and diCn:1PC bilayer properties.

MATERIALS AND METHODS

Synthetic diCn:1PCs (n=12-24) were purchased from Avanti Polar Lipids, C12NO prepared from *N*,*N*-dimethyldodecylamine by oxidation with hydrogen peroxide as described in [6] was kindly provided by Prof. F. Devínsky, CHOL was from Sigma, heavy water from Isotec and organic solvents (redistilled before use) from Slavus. Egg yolk phosphatidylcholine (EYPC) was isolated and purified as in [7].

Methods, chemicals and enzymes used for the SERCA isolation, purification, reconstitution into unilamellar diCn:1PC vesicles and estimation of its specific activity were described in detail in [7]. The amount of C12NO in the bilayer of SERCA+diCn:1PC vesicles was calculated from its sample concentration using the known molar partition coefficient between bilayers and aqueous phase determined recently [8]. Because of its high hydrophobicity, all the CHOL in the sample was located in the bilayers of SERCA+diCn:1PC vesicles.

For SANS experiments, weighted amounts of diCn:1PC, CHOL and C12NO were dissolved in chloroform and methanol mixtures. Appropriate volumes of these solutions were further mixed in glass tubes to achieve needed CHOL:diCn:1PC and C12NO:diCn:1PC molar ratios, the solvent was evaporated to dryness under a stream of pure gaseous N_2, followed by an oil-pump evacuation. The dry mass was dispersed at 1 wt. % concentration in heavy water under N_2 atmosphere by shaking, vortexing and ultrasonication. From the homogenized dispersions, unilamellar vesicles were prepared by extrusion through Nucleopore polycarbonate filters, with pores of diameter

50 nm, mounted in the Avestin LiposoFast Basic extruder fitted with two gas-tight Hamilton syringes. Each sample was subjected to 25-51 passes through filters at about 30°C. An odd number of passes were performed to avoid sample contaminations by large and oligolamellar vesicles, which might not have passed through the filters. The samples thus prepared were filled into Hellma 2 mm quartz cells, closed and stored at room temperature. As above, the amount of C12NO in the bilayer of vesicles was calculated using the known molar partition coefficient between bilayers and aqueous phase [8]. The maximum period between the sample preparation and its measurement was 5 h.

The neutron scattering experiments were performed on the PAXE spectrometer located at the end of the G5 cold neutron guide of the Orphée reactor (LLB CEA Saclay) and on the small-angle time-of-flight axially symmetric neutron scattering spectrometer YuMO at the IBR-2 fast pulsed reactor (FLNP JINR Dubna). In experiments, the normalized SANS intensity $I_{exp}(q)$ in cm^{-1} units as a function of the scattering vector modulus $q=4\pi\sin\theta/\lambda$ (2θ is the scattering angle and λ the wave-length of neutrons) was corrected for background effects using the heavy water as a blank.

For the evaluation of $I_{exp}(q)$ data, we used the strip-function model of the coherent neutron scattering length density distribution $\rho(z)$ taken perpendicularly to the bilayer surface [5]. In this model, the bilayer in unilamellar vesicles is divided into concentric strips with radii from the inner bilayer radius R_0 to the outer radius R_6. The methyl, methine and a part of methylene groups of diCn:1PC acyl chains are located in the region spanning two strips from R_2 to R_4, the dividing surface at R_3 is located in the bilayer center. In the region from R_2 to R_4, the value of $\rho(z)$ is constant. The strips from R_0 to R_2 and from R_4 to R_6 contain "dry" polar diCn:1PC head groups (including choline, phosphate, glycerol and acyl chain carbonyls), a some limited number of water molecules per one diCn:1PC molecule n_W, and the rest of diCn:1PC acyl chain methylene groups. The contribution of the head groups to $\rho(z)$ is triangular, increasing from R_0 (R_6) to R_1 (R_5) and decreasing then to R_2 (R_4). The contribution of water molecules to $\rho(z)$ decreases linearly from R_0 (R_6) to R_2 (R_4). Finally, the contribution of diCn:1PC acyl chain methylene groups not located in the strips between R_2 and R_4 decreases linearly from R_2 to R_1 and from R_4 to R_5. The fragmental molecular volumes of constituents in R_0 to R_2 and in R_4 to R_6 strips are additive and the decrease in volume due to one constituent is compensated by the increase due to another one. The steric bilayer thickness is equal to $d_S=R_6-R_0$. The partitioning of probability distributions for the lipid and an additive is done based on simple complementarity.

The experimental $I_{exp}(q)$ versus q data were fitted by the function minimization and error analysis program Minuit (CERN Program Library entry D506), using the vesicle structure factor derived for the strip model described above, convoluted by the Gamma function distribution of vesicle radii and by the SANS spectrometer resolution function. Besides the experimental $I_{exp}(q)$ data, the input values were the fragmental volumes of different parts of the bilayer obtained by densitometry [9-11] and the values of their coherent scattering amplitudes calculated by using the known tabulated scattering amplitudes of nuclei. During the minimization, the distances of $R_2-R_0=R_6-R_4$ were constrained to the value 1.2 nm obtained from molecular dynamics simulations [5]. The result of fitting is the mean vesicle outer radius and a parameter characterizing the radii distribution (not shown and discussed below), and a pair of d_S and n_W values; the surface area A_L of one diCn:1PC molecule + the appropriate fraction of CHOL or C12NO at the bilayer – aqueous phase interface is calculated from these d_S and n_W values using the known fragmental volumes of different parts of the bilayer.

Changes in the phosphatidylcholine head group conformation were followed by using the proton decoupled ^{31}P-NMR spectroscopy of multilamellar C12NO+EYPC vesicles. C12NO and EYPC were mixed at the needed molar ratio in chloroform/methanol in a glass tube; the solvent was evaporated under a stream of gaseous nitrogen and its traces removed by an oil vacuum pump. The dry EYPC+C12NO mixtures were transferred to other glass tubes and evacuated again. Redistilled water was added to these dry mixtures at the H_2O:EYPC=1:1 weight ratio, the amount of water added was controlled by gravimetry. Finally, the tubes were flame sealed, and the content was homogenized by repeated freezing and thawing and by forth-and-back centrifugation. Before the measurement, the samples were equilibrated at room temperature in a dark place. ^{31}P-NMR spectra were recorded on a Varian VXR 300 NMR spectrometer at 121.4 MHz using the deuterium lock, HF pulse width 45-55º and the interpulse relaxation delay 0.7-1.0 sec. The spectra were recorded using the strong proton inverse gated proton decoupling. The sample temperature was maintained at 25ºC using the gas-flow system of NMR spectrometer. Exponential multiplication of free induction decays corresponding to 50 Hz line broadening was applied prior to their Fourier transformation. The effective ^{31}P-NMR chemical shift anisotropy, $-\Delta\sigma_{eff}$, was evaluated as the distance between extremes of the first derivative spectra and corrected for the Lorentzian linewidth broadening using the computer simulated spectra..

RESULTS AND DISCUSSION

The specific SERCA ATPase activity reconstituted into fluid bilayers of unilamellar diCn:1PC vesicles is sensitive to the acyl chain length n with a maximum at n=18 (diC18:1PC) while phosphatidylcholines with shorter or longer acyl chains support progressively decreasing activities when approaching the chain length extremes (Fig. 1). In biochemical literature, this dependence is frequently explained by a hydrophobic mismatch hypothesis: It is supposed that the thickness of the bilayer hydrophobic region d_C must match the length of SERCA hydrophobic segments (α-helices) to support the maximum activity; increasing or decreasing this thickness should bring about SERCA conformation

changes and/or SERCA lateral aggregation resulting in the decreased ATPase activity and Ca^{2+} transport.

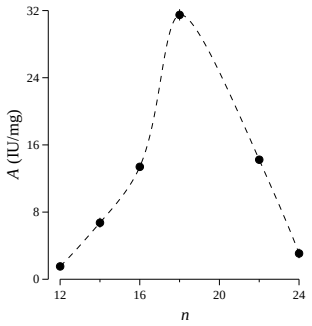

Fig. 1. Dependence of the SERCA specific ATPase activity *A* on the number *n* of diCn:1PC acyl chain carbon atoms. The dashed line was drawn to guide eye.

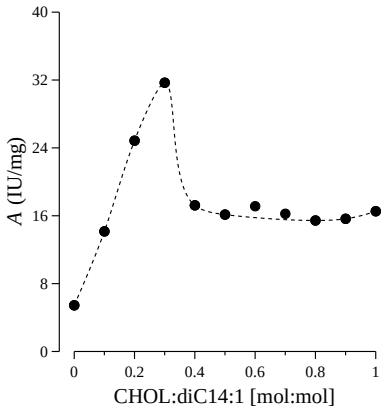

Fig. 2. Dependence of the SERCA specific ATPase activity *A* on the CHOL:diC14:1PC molar ratio.

When the SERCA protein is reconstituted into bilayers of diC14:1PC with suboptimal acyl chain lengths, the presence of CHOL in bilayers causes an increase in the ATPase activity up to CHOL:diC14:1PC=0.3 molar ratio; at higher molar ratios (≥0.4) the activity decreases to about one half of maximum level and fluctuates around the A=16.3±0.7 IU/mg value (Fig. 2). Finally, the ATPase activity of SERCA reconstituted into bilayers from diC18:1PC with optimal acyl chain lengths slightly increases when C12NO is admixed into bilayers (Fig. 3).

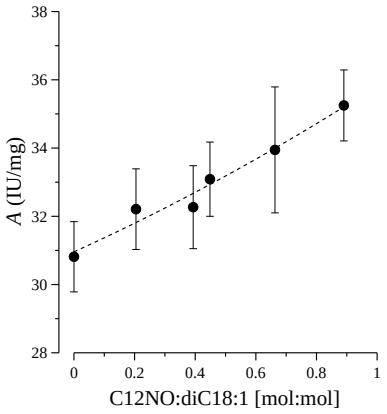

Fig. 3. Dependence of the SERCA specific ATPase activity *A* on the C12NO:diC18:1PC molar ratio.

To compare the SERCA ATPase specific activity changes with the bilayer structural parameters, we have studied the steric bilayer thickness d_S, the surface area A_L per lipid at the bilayer – aqueous phase interface and the number of water molecules n_W per lipid located in the polar region of bilayer of unilamellar diCn:1PC vesicles without and with CHOL and C12NO additives. Typical experimental dependencies of the scattered intensity $I_{exp}(q)$ on the scattering vector modulus q is shown in Fig. 4.

For a dispersion of unilamellar vesicles, which are approximately spherical in shape and monodisperse in size, the coherent scattered intensity is given by

$$I(q) = N\left|F(q)\right|^2 S(q) \qquad (1)$$

where N is the number of vesicles, $F(q)$ is the form factor of one vesicle and $S(q)$ is the intervesicle structure factor. The form factor is the Fourier transform of the contrast $\rho=\rho_L-\rho_w$ what is the difference of the coherent neutron scattering length density of the bilayer ρ_L and that of the aqueous phase ρ_w. The calculated interparticle structure factor for uncharged spherical particles which assumes their non-specific association (steric avoidance) is $S(q)\approx 1$ for $q\geq 0.1$ nm^{-1} [5]; Nawroth et al. [12] and Kiselev et al. [13] have found in experiment $S(q)=1$ for $q\geq 0.05$ nm^{-1} when the lipid concentration was less than 2 wt%. The extruded unilamellar vesicles are polydisperse in sizes; the coherent scattered intensity is then sum

$$I(q) = \sum_i N_i\left|F_i(q)\right|^2 \qquad (2)$$

over all vesicle sizes. This summation brings about a smearing of the fast $I(q)$ oscillations with the period π/R which would be observed in monodisperse vesicles with the radius R. In the experimental SANS curves (Fig. 4), only the first very shallow minimum at $q\sim 0.1$ nm^{-1} due these oscillations can be recognized. Solid lines in Fig. 4 correspond to the best fits as obtained using the advanced model of SANS data evaluation described in Materials and Methods.

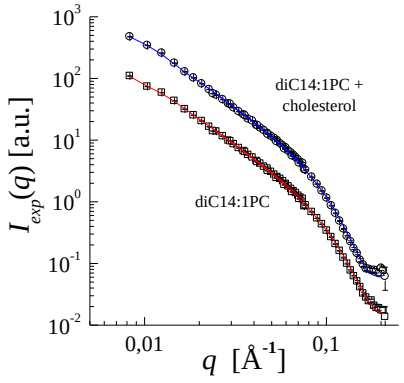

Fig. 4. Experimental SANS data obtained with unilamellar diC14:1PC vesicles without and with 33 mol% of CHOL. Scattering curves are shifted vertically for clarity of presentation.

As expected, we have found that the bilayer thickness of pure diCn:1PC bilayers without any additives increases with the increase of the acyl chain length n (Fig. 5). A simple linear fit gives d_S=(1.64±0.20)+(0.17±0.01)n in nm. Unexpectedly, the surface area A_L displays a maximum at n=18 and decreases for shorter and longer acyl chain lengths; the changes in A_L with the acyl chain length are accompanied by changes in the number of water molecules n_W located in the polar region of bilayer.

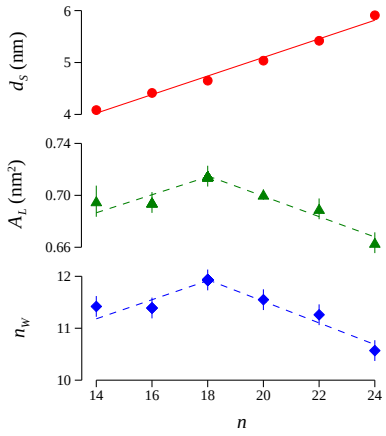

Fig. 5 Dependencies of steric thickness d_S, surface area A_L and number of water molecules per lipid n_W in diCn:1PC bilayers of unilamellar vesicles as a function of acyl chain length n.

Since the parameters in Fig. 5 were obtained at 30ºC and the SERCA ATPase activities in Fig. 1 at 37ºC, we have extrapolated the A_L and d_S data in Fig. 2 to 37ºC by correcting for temperature effects. The surface area was corrected using the lateral thermal expansivity $\beta=\partial(\ln A_L)/\partial T$= =0.003 K^{-1} as in [14], and the bilayer thickness by using the transversal thermal expansivity $\alpha=\partial(\ln d_S)/\partial T$= =0.001 K^{-1} found recently for diC18:1PC [15]. The steric bilayer thickness increases with the acyl chain length n as d_S=(1.66±0.20)+(0.17±0.01)n in nm at 37ºC – the change is rather small comparing to 30ºC. After temperature corrections, the surface area A_L is slightly higher, but the maximum at n=18 and the decrease for shorter and longer acyl chain lengths are observed at 37ºC too (not shown).

The biphasic A_L and n_W dependences on n were unexpected. Earlier, the decrease of A_L with the length of acyl chain has been observed in bilayers prepared from diacylphosphatidylcholines with saturated acyl chains (diCn:0PC) in multilamellar vesicles in the solid-like gel state for n=16-18 by small-angle X-ray diffraction (SAXD) [16], in multilamellar diCn:0PC vesicles in the fluid state for n=12–18 by ^{2}H NMR [17, 18] and in unilamellar diCn:0PC vesicles in the fluid state for n=10–18 by SANS [19]. The specific dependence of A_L (and n_W) on n in diCn:1PC bilayers in comparison to diCn:0PC bilayers could be caused by the presence and position of the double bond in the diCn:1PC acyl chains (Marrinck, personal communication). The value of lipid surface area A_L is the result of attractive and repulsive forces acting at the aqueous phase - bilayer interface. The main attractive components are the van der Waals forces between acyl chains and head group dipolar interactions, and the main repulsive components include steric interactions, hydration forces, and entropic contributions due to acyl chain ordering; the equilibrium area A_L is given by the balance of these forces that minimizes the interfacial free energy. At a constant temperature, the increase of acyl chain length will increase the van der Waals attraction and this will reduce the A_L value. However, the reduction of A_L will result at the same time in the reduction of *gauche* conformers formation in chains, decreasing thus the chain disorder (i.e. the entropy) and this could be dependent on the double bond position in the acyl chains. These two effects which act in opposite directions could cause the peculiar dependence of A_L (and n_W) in diCn:1PC bilayers observed. The value of A_L is thus a measure of lateral interactions in the bilayer. Irrespective of the actual mechanisms resulting in the chain length dependences of A_L and n_W, the results summarized in Fig. 5 indicate that not only the bilayer thickness but also the bilayer hydration and lateral interactions could influence the SERCA ATPase activity. Changes in lateral interactions will result in changes of bilayer lateral pressure profile suggested to affect conformations of membrane proteins [20,21]. Besides the "hydrophobic mismatch", this could be a mechanism contributing to the acyl chain dependence of the reconstituted SERCA ATPase activity.

To explain the biphasic effect of CHOL on the SERCA ATPase activity seen in Fig. 2, we have determined the effect of CHOL on the steric bilayer thickness of CHOL in unilamellar diC14:1PC vesicles using SANS and the evaluation method as above. The results are shown in Fig. 6. Though large experimental errors, it is seen that the bilayer steric thickness increases due to the presence of CHOL in diC14:1PC bilayers, reaching the value measured for diC18:1PC bilayers at CHOL:diC14:1PC=0.4 molar ratio and that for diC20:1PC bilayers at CHOL:diC14:1PC=0.4 molar ratio. It is commonly accepted that 3β-hydroxyl group of CHOL locates just below the lipid-aqueous interface and the steroid moiety orients in the hydrophobic interior of bilayer with its long molecular axis slightly tilted relative to the bilayer normal. The phospholipid acyl chain carbons in positions 2–10 have been estimated to lie in close proximity to the CHOL tetracyclic ring structure. The close proximity of the planar CHOL ring system orders the hydrocarbon chains and diminishes *trans–gauche* isomerization about their carbon–carbon bonds. As a consequence, the thickness of the bilayer increases which is confirmed by our results. Comparing the data in Fig. 1 and Fig. 6, one can conclude that cholesterol regulates the SERCA activity predominantly by influencing the bilayer thickness – when the thickness approaches the value supporting the maximum activity in diC18:1PC bilayers, the SERCA activity is maximal, further bilayer thickness increase results in the sudden activity decrease. This is however a rather crude picture not explaining why the activity data in Fig. 2 fluctuate around A=16.3±0.7 IU/mg value at CHOL:diC14:1PC≥0.4 molar ratio – one would expect a

continuous decrease in activity. Further studies will be needed to explain this effect, especially biochemical experiments with the SERCA protein reconstituted into mixed diC18:1PC+diC20:1PC bilayers to trace details in the activity dependence in the vicinity of its maximum.

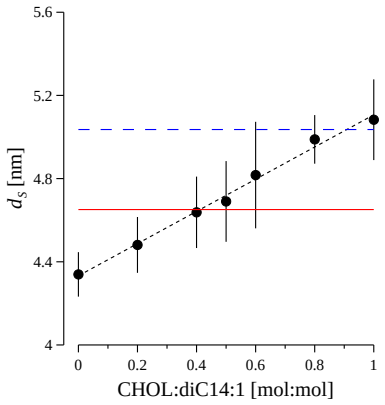

Fig. 6. Dependence of the steric bilayer thickness d_S as a function of CHOL:diC14:1PC molar ratio. The full horizontal line shows the d_S value for diC18:1PC bilayers and the dashed horizontal line that for diC20:1PC bilayers.

From the SANS data obtained with unilamellar vesicles, the bilayer steric thickness d_S has been obtained as a function of C12NO:diC18:1PC molar ratio as above. We have found that d_S decreases with the increase of molar ratio (not shown). The C12NO molecules incorporate into bilayer due to their amphiphilic properties. In the bilayer, the polar fragment of C12NO interacts with polar fragments of diC18:1PC and the C12NO alkyl chain with the diC18:1PC acyl chains. Due to the mismatch between lengths of C12NO and diC18:1PC chains, C12NO creates voids („free volume“) in the bilayer hydrophobic region, which is compensated by a *trans-gauche* isomerisation of alkyl and acyl chains or by their interdigitation. As a result, the bilayer steric thickness is decreased. Since the SERCA ATPase specific activity A is known as a function of C12NO:diC18:1 molar ratio (Fig. 3 and [7]), the activity can be then replotted as a function of bilayer thickness.

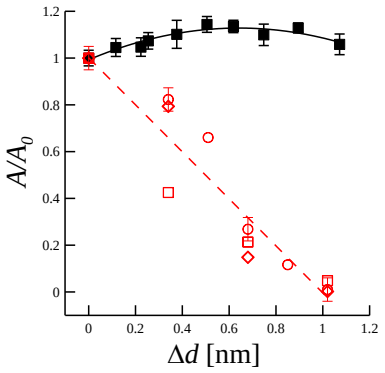

Fig. 7. Comparison of the normalized SERCA ATPase activity A/A_0 on the decrease of lipid bilayer thickness Δd. SERCA was reconstituted into C12NO+diC18:1PC bilayers (■) or into neat diCn:1PC bilayers (◇○□), the activity data were taken from Fig. 1 (□) and Fig. 3 (■) of the present paper, and from papers [22] (◇) and [23] (○).

Fig. 7 shows the normalized activity A/A_0 as a function of bilayer thickness decrease Δd, where A is the activity measured at the bilayer thickness d_S and A_0 the activity measured at the thickness d_{S0}, the thickness d_{S0} being the steric thickness of neat diC18:1PC bilayers in unilamellar vesicles (Fig. 5); the thickness decrease is defined as $\Delta d = d_S - d_{S0}$. The plot of A/A_0 vs. Δd is convenient for a comparison of activity data at the same Δd but induced by different mechanisms. In Fig. 7, we compare the A/A_0 data obtained with the *SERCA* protein reconstituted into C12NO:diC18:1PC bilayers (Fig. 3 and [7]) with those obtained with the *SERCA* protein reconstituted into fluid bilayers from neat diCn:1PCs. It can be seen that the effect of bilayer thickness decrease, which otherwise results in the activity decrease in neat diCn:1PC bilayers without any additives, must be compensated by some other factors.

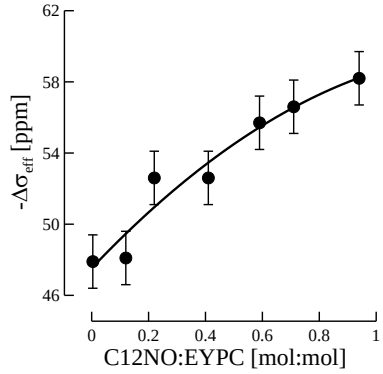

Fig. 8. Dependence of the ^{31}P-NMR chemical shift anisotropy $-\Delta\sigma_{eff}$ on the C12NO:EYPC molar ratio in multilamellar vesicles.

One of these factors follows from the results of ^{31}P-NMR experiments with C12NO:EYPC multilamellar vesicles (Fig. 8). EYPC is a natural phospholipid which average chemical composition is very close to diC18:1PC (see [11] and references therein). In the C12NO:EYPC molar ratio interval where the SERCA ATPase activity increases (Fig. 3), a parallel increase in the effective ^{31}P-NMR chemical shift anisotropy, $-\Delta\sigma_{eff}$, is observed. Changes in the $-\Delta\sigma_{eff}$ anisotropy have been observed earlier in phosphatidylcholine bilayers interacting with metal cations and amphiphilic anionic, cationic and dipolar substances, and have been ascribed to the change in the phospholipid head-group conformation [24]: When the N^+-P^- dipole of phosphatidylcholines moves with its N^+ end toward the perpendicular direction to the bilayer, the axis of the chemical shift tensor coinciding with the vector connecting the two esterified oxygens of the phospholipid phosphate group reorients in the same direction and this causes the increase in anisotropy. Seelig [25] calculated that the N^+-P^- dipole reorientation is accompanied by variations of the local membrane dipole potential of the order of 10^5 V/cm and suggested that this could play a regulatory role in membrane function. Cafiso [26] suggested that changes in membrane dipole potentials could affect membrane protein conformation. It is possible, that the N^+-P^- dipole

of diC18:1PC reorientation induced by C12NO could be thus a factor compensating the influence of the bilayer thickness decrease on the SERCA ATPase activity.

CONCLUSIONS

The lipid bilayer thickness must be measured in order to understand the function of integral membrane proteins. A convenient method of bilayer thickness measurements is the small-angle neutron scattering on unilamellar lipid vesicles combined with the advanced models of data evaluation.

ACKNOWLEDGMENT: This study was supported by the APVV-51-027404 and VEGA 1/3029/06 and 1/2280/05 grants, by the JINR Dubna project 07-4-1031-99/2008, and by the European Commission under the 6th Framework Programme through the Key Action: Strengthening the European Research Area, Research Infrastructures, Contract № RII3-CT-2003-505925. The authors thank Prof. Ing. F. Devínsky, DrSc. Dr.h.c. for providing the C12NO chemical.

REFERENCES

1. O.G. Mouritsen: Life – As a Matter of Fat; The Emerging Science of Lipidomics (Springer, Berlin and Heidelberg – 2005).
2. Y.F. Liu, J. F. Nagle: Phys. Rev. E **69**, 040901 (2004).
3. N. Kučerka, Y.F. Liu, N.J. Chu, H.I. Petrache, S.T. Tristram-Nagle, J.F. Nagle: Biophys. J. **88**, 2626 (2005).
4. N. Kučerka, M. A. Kiselev, P. Balgavý: Eur. Biophys. J. **33**, 328 (2004).
5. N. Kučerka, J.F. Nagle, S.E. Feller, P. Balgavý: Phys. Rev. E 69, 051903 (2004).
6. F. Devínsky, I. Lacko, A. Nagy and L. Krasnec: Chem. Zvesti **32**, 106 (1978).
7. J. Karlovská, D. Uhríková, N. Kučerka, J. Teixeira, F. Devínsky, I. Lacko, P. Balgavý: Biophys. Chem. 119 (2006) 69
8. J. Karlovská, F. Devínsky, P. Balgavý: Gen. Physiol. Biophys., in press (2007).
9. L. Benjamin: J. Phys. Chem. **70**, 3790 (1966).
10. A.I. Greenwood, S. Tristram-Nagle, J.F. Nagle: Chem. Phys. Lipids **143**, 1 (2006).
11. D. Uhríková, P. Rybár, T. Hianik, P. Balgavý: Chem. Phys. Lipids **145**, 97 (2007).
12. T. Nawroth, H. Conrad, K.Dose: Physica B **156&157**, 477 (1989).
13. M.A. Kiselev, D. Lombardo, A.M. Kisselev, P. Lesieur: In: JINR Annual Report 2000 (Eds. A.V. Belushkin and V.V. Sikolenko), FLNP JINR, Dubna, Russia, 2001, p. 136.
14. S. Tristram-Nagle, H.I. Petrache, J.F. Nagle: Biophys. J. **75**, 917 (1998).
15. D. Uhríková, M. Hanulová, S. S. Funari, R. S. Khusainova, F. Šeršeň, P. Balgavý: Biochim. Biophys. Acta **1713**, 15 (2005).
16. W.J. Sun, S. Tristram-Nagle, R.M. Suter, J. F. Nagle: Biophys. J. **71**, 885 (1996).
17. M.R. Morrow, J.P. Whitehead, D. Lu: Biophys. J. **63**, 18 (1992).
18. H.I. Petrache, S.W. Dodd, M.F. Brown: Biophys. J. 79, 3172 (2000).
19. P. Balgavý, M. Dubničková, N. Kučerka, M.A. Kiselev, S.P. Yaradaikin, D. Uhríková: Biochim. Biophys. Acta **1512**, 40 (2001).
20. R.S. Cantor: Chem. Phys. Lipids **101**, 45 (1999).
21. R.S. Cantor: Biophys. J. **80**, 2284 (2001).
22. A.G. Lee, J.M. East, P. Balgavý: Pesticide Sci. **32**, 317 (1991).
23. A. Johannsson, C.A. Keightley, G.A. Smith, C.D. Richards, T.R.Hesketh, J.C. Metcalfe: J. Biol. Chem. **256**, 1643 (1981).
24. P.G. Scherer, J. Seelig: Biochemistry **28**, 7720 (1989).
25. J. Seelig: Cell Biol. Int. Rep. **14**, 353 (1990).
26. D. S. Cafiso: Toxicol. Lett. **100-101**, 431 (1998).